ORIGINAL ARTICLE

INTERNATIONAL JOURNAL OF RESEARCH IN PHARMACEUTICAL SCIENCES

Published by JK Welfare & Pharmascope Foundation Journal Home Page: www.ijrps.com

Development of n-HA/CS-GM biomimetic nanocomposite for biomedical applications

Aswathy C, Jenson Samraj J, Gurusamy Annadurai*

Department of Environmental Sciences, Sri Paramakalyani Centre for Excellence in Environmental Sciences, Manonmaniam Sundaranar University, Alwarkurichi, Tamil Nadu - 627412, India

Article History:

Received on: 08 Sep 2021
Revised on: 03 Oct 2021
Accepted on: 08 Oct 2021

Keywords:

Osteomyelitis, Nanohydroxyapatite, Guar gum, Co-precipitation, Osteosarcoma

ABSTRACT

Nowadays, effective treatment and management of malignant osteomyelitis remain an alarming clinical challenge causing the creation of antimicrobial biomaterials for orthopedic surgeons. The has revived attention in creating antimicrobial biomaterials for orthopedics. The collaboration of nanotechnology and engineered biomaterials will probably provide perception for developing novel and hybrid composites. Because of improved control of the interaction between nanoparticles and polymers, nanohydroxyapatite (n-HA) incorporated nanocomposite would provide versatility in designing specific properties. As a result, the study describes the ethanolic extraction of Guar gum from native *Cassia fistula* seeds, as well as the development of (n-HA), Chitosan (CS) and Guar gum (GM) nanocomposite via the Co-precipitation method. The nanocomposites were characterized based on their physico-chemical and morphological properties, such as XRD, FT-IR and SEM. The nanocomposites were tested for antibacterial activity against *Staphylococcus aureus(S.aureus)* ATCC25923 and anticancer activity against MG 63 (osteosarcoma) cancer cell line MTT assay. The antibacterial result confirms that the n-HA/CS-GM hybrid nanocomposites exhibit excellent antibacterial properties against *Staphylococcus aureus* and average inhibition zones of the different content samples against *S. aureus* were 15.75 mm for n-HA/CS and 19.75 mm for n-HA/CS-GM hybrid microspheres, respectively. The cytotoxicity result showed that the average OD of cells treated with 7.8 to 1000 μg/mL concentration of n-HA/CS composite varied from 0.479 to 0.297 parallel to 88.70% to 55% cell viability and the OD of n-HA/CS-GM composite varied from 0.447 to 0.273 corresponding 82.77% to 50.55% cell viability for 7.8μg/mL concentration up to 1000μg/mL.

*Corresponding Author

Name: Gurusamy Annadurai
Phone: +91-9442027196
Email: gannadurai@msuniv.ac.in

ISSN: 0975-7538

DOI: https://doi.org/10.26452/ijrps.v13i1.15

Production and Hosted by

IJRPS | www.ijrps.com

INTRODUCTION

Osteomyelitis was a rare disease to the human bone where the serious condition can cause severe infection on a bone, especially from an infecting organism. Although bones are normally resistant to bacterial colonization, events such as trauma, surgery, the presence of foreign bodies, or the placement of prostheses may disrupt bone integrity and lead to the onset of bone infection [1]. Bacteria causing osteomyelitis can invade the bone-forming osteoblasts, lead to pervasive inflammation necrosis and finally lead to bone destruction [2, 3].

*S.aureus*is, the most common causative pathogen, is causing chronic osteomyelitis. The contemporary osteomyelitis treatment strategy includes surgical debridement and systemic antimicrobial therapy, which cause higher antibiotic concentrations at the infected site [4]. However, complete inhibition of bacteria at the infected site remains unsuccessful as they gradually colonize and forms biofilms leading to tumor growth [5]. Active treatment of chronic osteomyelitis employing antimicrobial agents remains a significant clinical challenge. Furthermore, an increasing number of osteomyelitis cases are due to multiple infections or multidrug resistant bacterial strains such as methicillin-resistant *S. aureus* [6]. The enhanced permeability and retention (EPR) effect caused by the inflamed tissues enables nanomedicine to find a better way for treating the infection [7, 8]. Hence engineered nanomaterials with osteoinductive moieties as drug carriers are expected as the most promising strategy used by orthopedics for tissue engineering and regeneration [9]. A vast range of nanocomposite formulations of hydroxyapatite is in use for drug delivery systems for hard tissue engineering applications. [10], for the first time, reported the bioinspired fabrication of carbonated hydroxyapatite/CS (CHA/CS) nanohybrid scaffolds for regeneration in rat cranial defect models. These nanohybrid scaffolds exhibited a prominent capacity in promoting intrinsic bone regeneration. Numerous studies have reported the properties of natural gums and modified natural gums as promising biodegradable polymers for drug delivery and orthopedics applications [11, 12]. Another study by [13] reported the preparation and properties of a novel bone repair composite: nano-hydroxyapatite/CS/carboxymethyl cellulose and the results showed that n-HA particles were dispersed uniformly in the organic phase with strong chemical interactions formed among the three phases and also the composites were similar to natural bone in morphology and size [14].

Nano-hydroxyapatite (n-HA) is a bioactive, biocompatible and bioresorbable nanoceramic material exhibiting both osteoconductive and osteoinductive properties and interacts with the natural tissue without evoking any inflammatory response [15–17]. Owing to its similitude with human hard tissue, it was referred to as biological apatite. Moreover, hydroxyapatite nanoparticles can be made from distinct and customized synthetic methods to improve their physical-chemical properties and reduce their cytotoxicity in biological systems [18, 19]. In particular, it is an assuring material for discrete hard tissue engineering applications. The addition of small quantities of n-HA can rigorously enhance the mechanical characteristics of the polymer matrix [20]. Numerous studies reported the nanocomposite formulations as drug carriers for tissue engineering applications. Moreover, Huang *et al*. (2020) evaluated the effects of composite materials on tumor growth inhibition and bone growth induction using strontium/CS/hydroxyapatite/norcantharidin composite.

In this study, we report the synthesis of n-HA/CS and n-HA/CS-GM nanocomposites by the co-precipitation method. The synthesized nanocomposites were further characterized using XRD (X-ray diffraction), Fourier transform infrared (FT-IR) spectroscopy and scanning electron microscopy (SEM). Notably, the nanocomposite with GM extracted from *Cassia fistula* seeds showed a great impact on tumor cell inhibition and higher antibacterial activity compared to the CSn-HA composite.

MATERIALS AND METHODS

Chemicals and reagents

The calcium nitrate tetrahydrate purified ($Ca(NO_3)_2.4H_2O$), Diammonium Hydrogen Orthophosphate ($(NH_4)_2HPO_4$, CS and other chemicals and reagents were purchased from Hi-media Mumbai, India.

Synthesis of Hydroxyapatite nanoparticles

Hydroxyapatite nanoparticles were synthesized by a wet chemical method with slighter modifications. For that, 500 ml of 0.4 mol of diammonium hydrogen phosphate ($(NH_4)_2HPO_4$(pH4.0) was vigorously stirred in a 2 L beaker at room temperature and 500 mL of 0.6 mol calcium nitrate tetrahydrate (pH7.4) was added drop wise over 4 h. The pH of the system was maintained at 10.8 throughout the stirring process by using 0.1 M sodium hydroxide. The mixture was allowed to remain stirred overnight. The formation of white precipitate was cleaned with distilled water and ethanol simultaneously about 3 to 4 times. Then the precipitate was dried in a hot air oven for 5 hours and sintered at 650^0C for 2 hours to get pure n-HA powder.

Guargumextraction and purification

Cassia fistula fruit was collected from our campus and their seeds were removed manually. Whole seeds are sun-dried and dry weight was measured using an electronic balance and further soaked in water overnight at room temperature. The seed coat and germs were separated manually and left to air dry and the percentage of whole seed weight was calculated. A known weight of endosperm was

dispersed in water (1:5 ratio) blended in a kitchen blender and autoclaved, followed by centrifugation at 6000 rpm for 60 min. Then the supernatant was filtered using ethanol (99%), a white slimy precipitate was obtained, the precipitate was retreated with acetone and dissolved in 50 ml of hot water and again reprecipitated with acetone and ethanol several times until a fibrous particle was obtained. The purified sample was collected and dried at 65°C in an oven for 24 hours. The dried polysaccharide was weighed and stored in an air-tight container [21–23].

Synthesis of n-HA/CS-GM composite

The nano-hydroxyapatite/CS-GM (n-HA/CS-GG) nanocomposites were synthesized via the co-precipitation method at room temperature. A blend of CS-GM (CS-GM) with a concentration of 3% (W/V) was prepared. CS (CS) was dissolved in 100 ml of 1% (WV) aqueous acetic acid solution with stirring for 24 hours to get a clear solution. Simultaneously, GM was dissolved in 100 ml of double-distilled water at 55 ºC with stirring for 12 hours. The two polymer solutions were mixed under agitation until the solution mixture was homogeneous. In addition, nano-hydroxyapatite(n-HA) suspension was prepared by dispersing synthesized n-HA powder in 100 ml of double-distilled water in a sonicator water bath for 3 hours. The dispersed n-HA particles were added to the CS-GG blend drop-by-drop while stirring vigorously. The pH of the mixture was maintained with freshly prepared 1M NaOH solution up to ~11. The stirring was continued for 24 hours to ensure homogeneous mixing and then left undisturbed for 48 hours ageing, resulting in a creamish white precipitate. After that, the precipitate was filtered and rinsed several times with deionized water until the pH of the elute gets neutralized and oven-dried at 70ºC. Finally, the resultant dried cake was grounded to obtain fine powders [24, 25].

Agar well diffusion assay for antibacterial tests

The biocidal performance of n-HA/CS/GM nanocomposites was conducted by Agar well diffusion method. The major bacterial strain causing osteomyelitis, Gram-positive (*S. aureus*) microorganisms, were obtained from SPKCES-MS University campus, Alwarkurichi, India. Stock cultures were maintained at 4 agar slants of nutrient media. Before the experiment, pure cultures were sub-cultured onto Muller Hinton broth and incubated overnight at 37°C [26, 27]. Later Muller Hinton agar plates were swabbed with cultures using a sterile cotton swab and punctured for wells. After that, the test samples were inoculated into 7mm wells at different concentrations. After 24 h of incubation, Zone of Inhibition (ZOI) was measured [28, 29].

MTT assay

Cytotoxicity of the synthesized nanocomposites was evaluated by MTT assay on MG 63 cells isolated from osteosarcoma affected bone tissue.1x10^{5}cells/mL were seeded into 24 well plates and incubated in 35^{o}C with 5% CO_2 condition for 24 hours. After incubation, the sample was removed from the well and washed with phosphate-buffered saline (pH 7.4) or DMEM without serum. 100μl/well (5mg/ml) of 0.5% 3-(4,5-dimethyl-2-thiazolyl)-2,5-diphenyl-tetrazolium bromide (MTT) was added and incubated for 4 hours. After incubation, 1ml of DMSO was added to all the wells. The absorbance at 570nm was measured with a UV- Spectrophotometer using DMSO as the blank [30]. Measurements were performed and the concentration required for a 50% inhibition (IC50) was determined graphically. The % cell viability was calculated using the following formula,

$$\%\ Cell\ viability\ = \frac{A570\ of\ treated\ cells}{A570\ of\ control\ cells} \times 100$$

RESULTS AND DISCUSSION

Characterization of nanocomposites

X-Ray Diffraction analysis (XRD)

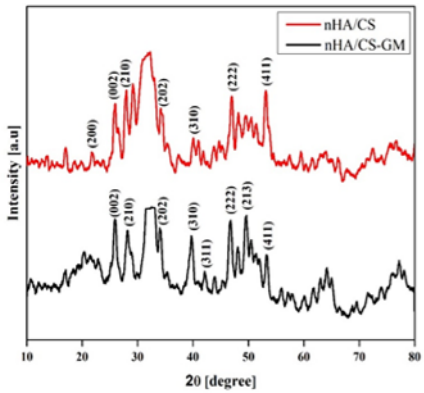

Figure 1: XRD spectrum of the synthesized n-HA/CS and n-HA/CS-GM nanocomposite

The XRD spectrum for n-HACS and n-HACS guar composites is depicted in Figure 1. The results suggest that the obtained composites are amorphous. From the X-ray diffractogram, the average crystalline sizes of the n-HA/CS and n-HA/CS-GM composites were 9.32 and 4.48 (nm). The n-HA/CS composite exhibited characteristic peaks at 2θ values of 21.87°, 25.95°, 28.96°, 34.10°, 39.83°, 46.76°, 53.21° are assigned to the carbonate hydroxyapatite planes of (200), (002), (210), (202), (310),

(222) and (411) respectively (JCPDS card no: 00-021-0145) (Brophy and Nash, 1968). On the other hand, n-HA/CS-GM composite exhibited characteristic peaks at 25.95°, 28.96°, 34.10°, 39.83°, 42.01°, 46.76° and 53.21° could be assigned to the carbonate hydroxyapatite planes of (002), (210), (202), (310), (311), (222), (213) and (411) respectively consisting of hexagonal crystal structure. This indicates that the amorphous particles of n-HA/CS-GM are very much incorporated on n-HA/CS substrate.

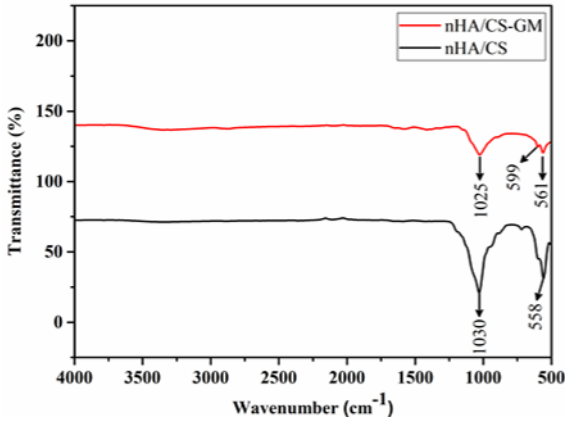

Figure 2: FT-IR spectrum of the synthesized n-HA/CS and n-HA/CS-GM nanocomposite

Fourier-transform infrared spectroscopy analysis (FT-IR)

The IR spectrum of n-HA/CS and n-HA/CS-GM composites is shown in Figure 2. The peaks of both the composites are observed in the far IR and IR region (500-1030 cm^{-1}). Interestingly, there are no distinct functional groups observed in both the composite materials, which may indicate the presence of hydrocarbon. The peaks of n-HA/CS composite at 1030 cm^{-1}, 558 cm^{-1} and the peaks of n-HA/CS-GM composite at 1025 cm^{-1} and 561 cm^{-1} may attribute to the presence of the phosphate group. Bands at 558cm^{-1},599 cm^{-1},561 cm^{-1} corresponds to C-I stretch. The peaks appeared in the spectrum of the GM between 800 and 1200 cm^{-1} of the highly coupled C- C- O, C-OH and C-O-C stretching modes of polymer shifted to a lower wave number when the GM mixed with n-HA/CS composite. In addition, the broadband formed between 3250cm^{-1} and 3400cm^{-1} seen in GM corresponding to polymeric OH stretch also disappeared. From the IR patterns, the specific peaks of pure n-HA appear in the spectrum of n-HA/CS and n-HA/CS-GM composites with band-shifts and peak decrease [31].

Scanning Electron Microscopy (SEM) analysis

The morphology of the n-HA/CS composite was flaky, revealing its layered structure with a flower petals-like appearance as shown inFigure 3 (a) and

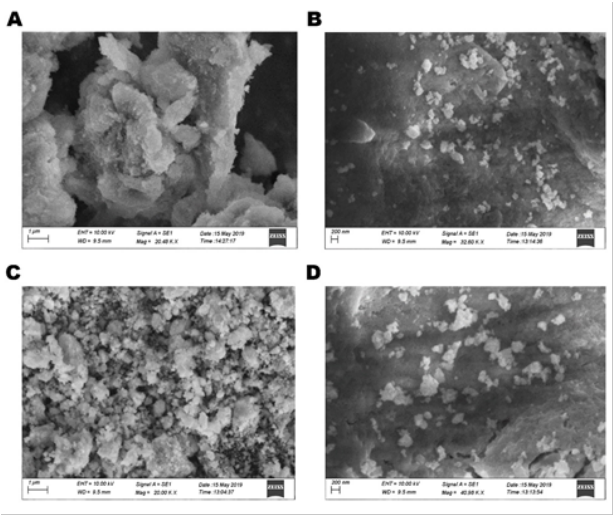

Figure 3: SEM images of then-HA/CS (a and b) and n-HA/CS-GM nanocomposite (c and d)

(b) and the n-HA/CS-GM composites have an undefined aggregated composition Figure 3(c) and (d) n-HA/CS-GM composites display a more distributed and dense structure compared to n-HA/CS composite as shown in Figure 3(D)The scanning electron micrographs of n-HA-CS and n-HA/CS-GM composites displayed randomly embedded n-HA in the polymer matrix with a modest level of agglomeration [14, 32, 33].

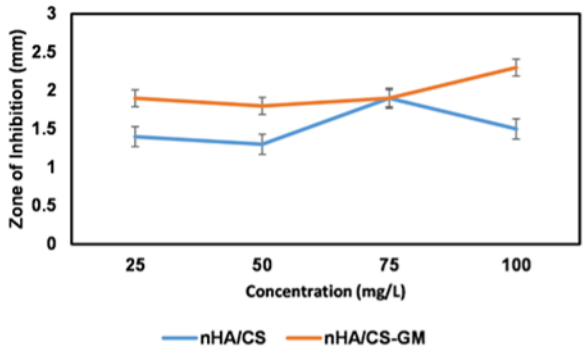

Figure 4: Antibacterial activity of the synthesized n-HA/CS and n-HA/CS-GM nanocomposite

Antibacterial studies

Figure 4 depicts n-HA/CS-GM nanocomposites against *S.aureus*. Various concentrations of n-HA/CS-GM inhibit bacterial growth. The zone formation around the disc clearly shows bacterial inhibition. The study confirms that the antibacterial activity of n-HA/CS-GM is greater than n-HA/CS composite. The result confirms the n-HA/CS-GM hybrid nanocomposites exhibit excellent antibacterial properties against *Staphylococcus aureus*. The average inhibition zones of the different content samples against *S. aureus* were 15.75 mm for

n-HA/CS and 19.75 mm for n-HA/CS-GM hybrid microspheres, respectively. The bacterial inhibition increased by the addition of GM. The result implies that n-HA/CS-GM composite was more efficient than n-HA/CS composite for restraining bacterial growth.

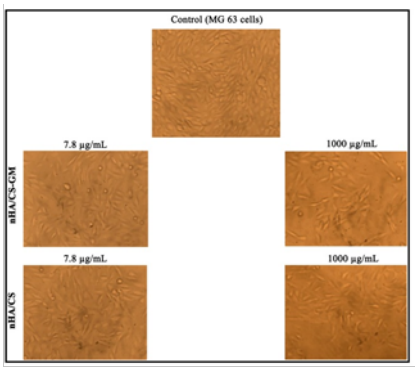

Figure 5: Anticancer effects of n-HA/CS and n-HA/CS-GM nanocomposite on MG-63 cell line

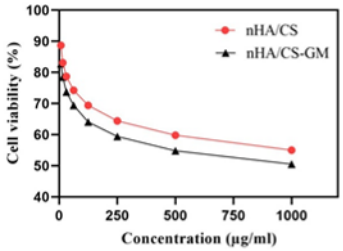

Figure 6: The anticancer effect of n-HA/CS and n-HA/CS-GM nanocomposite on MG-63 cell line

In vitro MTT assay

In the present work, the anticancer activity of n-HA/CS and n-HA/CS-GM composites was investigated on the MG-63 cell line, as depicted in Figure 5. Numerous studies have reported the tumor inhibition potential of n-HA composites. The average OD of cells treated with 7.8μg/mL -1000μg/mL concentration of n-HA/CS composite varies from 0.479to 0.297 parallel to 88.70% to 55% cell viability and the OD of n-HA/CS-GM composite varies from 0.447 to 0.273 corresponding 82.77%to 50.55% cell viability for 7.8μg/mL concentration up to1000μg/mL.On MG 63 cells, the n-HA/CS-GM composites had greater anti-proliferative efficacy than the other composites, as depicted in Figure 6. Therefore, these results suggest that the n-HA/CS-GM composites acted as anticancer agents at maximum concentrations. It is possible to increase the anti-proliferation of the malignant cells using the biocompatible n-HA/CS-GM composites with slight modifications. The cytotoxicity caused by the n-HA/CS-GM composite attributes involvement of oxidative stress, alterations in mitochondrial membrane potential and reduction of antioxidant potential eventually led to apoptosis and cell death.

CONCLUSIONS

Although there is no research on using GG-based ternary nanocomposite with CS and nano-hydroxyapatite for bone tissue engineering and bone infections, we have synthesized n-HA/CS and n-HA/CS-GM composites by the co-precipitation technique. The ceramic-polymer composites were assessed for anticancer studies on MG-63 cell lines. SEM micrographs of the composites obtained by combining n-HA in the CS and GM matrix confirmed the random dispersion of n-HA on the polymer matrix with undefined morphologies. XRD characterizations indicate the amorphous nature of n-HA/CS and n-HA/CS-GM composites. n-HA/CS-GM composites showed higher antibacterial activity on *S.aureus*than n-HA/CS nanocomposites. Anticancer activity against the MG-63cell line was investigated on n-HA/CS-GM nanocomposites that displayed slightly higher cytotoxicity on osteosarcoma cells than n-HA/CS composites. Overall, the n-HA/CS-GM nanocomposite exhibited a higher degree of anticancer activity, which could be a promising attempt for further improvement in malignant osteomyelitis treatment applications.

ACKNOWLEDGEMENT

Myself, C. Aswathy (Register no: 19214542272006), acknowledge the Research Centre Sri Paramakalyani Centre for Excellence in Environmental Sciences, Manonmaniam Sundaranar University, Alwarkurichi, for providing the support for this research work.

Funding Support

The authors declare that they have no funding support for this study.

Conflict of Interest

The authors declare that they have no conflict of interest.

REFERENCES

[1] S Kishner. Osteomyelitis: Background, Anatomy, Pathophysiology. *Medscape*, 2018. Updated On: 12 Jul 2020.

[2] S L Weimer, R F Wideman, C G Scanes, A Mauromoustakos, K D Christensen, and Y Vizzier-Thaxton. Impact of experimentally induced bacterial chondronecrosis with osteomyelitis (BCO) lameness on health, stress, and leg

health parameters in broilers. *Poultry Science*, 100(11):101457–101457, 2021.

[3] Z Zhou, Y Chen, H S Min, Y Wan, H Shan, Y Lin, W Xia, F Yin, C Jiang, and X Yu. Merlin functions as a critical regulator in Staphylococcus aureus-induced osteomyelitis. *Journal of Cellular Physiology*, pages 21–9541, 2021.

[4] D Gomes, M Pereira, and A F Bettencourt. Osteomyelitis: an overview of antimicrobial therapy. Braz. *J. Pharm. Sci*, 49(1):13–27, 2013.

[5] J M Fritz and J R Mcdonald. Osteomyelitis: Approach to Diagnosis and Treatment. *The Physician and Sportsmedicine*, 36(1):50–54, 2008.

[6] V Silago, M F Mushi, B A Remi, A Mwayi, S Swetala, C I Mtemisika, and S E Mshana. Methicillin-resistant Staphylococcus aureus causing osteomyelitis in a tertiary hospital. *Journal of Orthopaedic Surgery and Research*, 15(1), 2020.

[7] Y Nakamura, A Mochida, P L Choyke, and H Kobayashi. Nano drug Delivery: Is the Enhanced Permeability and Retention Effect Sufficient for Curing Cancer? *Bioconjugate Chemistry*, 27(10):2225–2238, 2016.

[8] T Shukla, N Upmanyu, S P Pandey, and M S Sudheesh. Site-specific drug delivery, targeting, and gene therapy. *Nanoarchitectonics in Biomedicine*, pages 473–505, 2019.

[9] F R Maia, S J Bidarra, P L Granja, and C C Barrias. Functionalization of biomaterials with small osteoinductive moieties. *Acta Biomaterialia*, 9(11):8773–8789, 2013.

[10] Y Chen, J Yu, Q Ke, Y Gao, C Zhang, and Y Guo. Bioinspired fabrication of carbonated hydroxyapatite/chitosan nanohybrid scaffolds loaded with TWS119 for bone regeneration. *Chemical Engineering Journal*, 341:112–125, 2018.

[11] T R Bhardwaj, M Kanwar, R Lal, and A Gupta. Natural Gums and Modified Natural Gums as Sustained-Release Carriers. *Drug Development and Industrial Pharmacy*, 26(10):1025–1038, 2000.

[12] C Tian, P Xu, J Jiang, and C Han. Preparation and drug-delivery study of functionalized hydroxyapatite based on natural polysaccharide gums with excellent drug-loading properties. *Journal of Dispersion Science and Technology*, 42(5):751–759, 2021.

[13] J Liuyun, L Yubao, Z Li, and L Jianguo. Preparation and properties of a novel bone repair composite: nano-hydroxyapatite/chitosan/carboxymethyl cellulose. *Journal of Materials Science: Materials in Medicine*, 19(3):981–987, 2008.

[14] Osteomyelitis. Genetic and Rare Diseases Information Center (GARD) - an NCATS Program. 2016. Updated On: 19 Oct 2016.

[15] K P Sanosh, M. C Chu, A Balakrishnan, Y. J Lee, T N Kim, and S. J Cho. Synthesis of nano-hydroxyapatite powder that simulates teeth particle morphology and composition. *Current Applied Physics*, 9(6):1459–1462, 2009.

[16] K Lin and J Chang. Structure and properties of hydroxyapatite for biomedical applications. *Hydroxyapatite (Hap) for Biomedical Applications*, pages 3–19, 2015.

[17] S Inthong, T Tunkasiri, S Eitssayeam, K Pengpat, and G Rujijanagul. Physical properties and bioactivity of nanocrystalline hydroxyapatite synthesized by a co-precipitation route. *Ceramics International*, 39:533–536, 2013.

[18] S Balu, S Kumar, Andra, and J Jeevanandam. Emerging marine-derived nanohydroxyapatite and their composites for an implant and biomedical applications. *J Mech Behav Biomed Mater*, 119:104523–104523, 2021.

[19] M Du, J Chen, K Liu, H Xing, and C Song. Recent advances in biomedical engineering of nano-hydroxyapatite include dentistry, cancer treatment and bone repair. *Composites Part B: Engineering*, 215, 2021.

[20] M R Nikpour, S M Rabiee, and M Jahanshahi. Synthesis and characterization of hydroxyapatite/chitosan nanocomposite materials for medical engineering applications. *Composites Part B: Engineering*, 43(4):1881–1886, 2012.

[21] M Shakir, I Zia, A Rehman, and R Ullah. Fabrication and characterization of nanoengineered biocompatible n-HA/chitosan-tamarind seed polysaccharide: Bio-inspired nanocomposites for bone tissue engineering. *International Journal of Biological Macromolecules*, 111:903–916, 2018.

[22] V Singh, R Sethi, and A Tiwari. Structure elucidation and properties of a non-ionic galactomannan derived from the Cassia pleurocarpa seeds. *International Journal of Biological Macromolecules*, 44(1):9–13, 2009.

[23] H Bhatia, P K Gupta, and P L Soni. Structure of the oligosaccharides isolated from Prosopis juliflora (Sw.) DC. Seed polysaccharide. *Carbohydrate Polymers*, 101:438–443, 2014.

[24] K S Katti, D R Katti, and R Dash. Synthesis and characterization of a novel chitosan/montmorillonite/hydroxyapatite

nanocomposite for bone tissue engineering. *Biomedical Materials*, 3(3), 2008.

[25] J Li, H Sun, D Sun, Y Yao, F Yao, and K Yao. Biomimetic multicomponent polysaccharide/nano-hydroxyapatite composites for bone tissue engineering. *Carbohydrate Polymers*, 85(4):885–894, 2011.

[26] DB Thomas and A Chinsamy. Chemometric analysis of EDXRF measurements from fossil bone. *X-ray Spectrom*, 40(6):441–445, 2011.

[27] R Sankar, A Karthik, A Prabu, S Karthik, K S Shivashangari, and V Ravikumar. Origanum vulgare mediated biosynthesis of silver nanoparticles for its antibacterial and anticancer activity. *Colloids and Surfaces B: Biointerfaces*, 108:80–84, 2013.

[28] G S Dhillon, S Kaur, and S K Brar. Facile fabrication and characterization of chitosan-based zinc oxide nanoparticles and evaluation of their antimicrobial and antibiofilm activity. *International Nano Letters*, 4(2):107–107, 2014.

[29] D Mubarakali, N Thajuddin, K Jeganathan, and M Gunasekaran. Plant extract mediated synthesis of silver and gold nanoparticles and its antibacterial activity against clinically isolated pathogens. *Colloids and Surfaces B: Biointerfaces*, 85(2):360–365, 2011.

[30] M K Ediriweera, K H Tennekoon, and S R Samarakoon. In vitro assays and techniques utilized in anticancer drug discovery. *Journal of Applied Toxicology*, 39(1):38–71, 2019.

[31] A B D Nandiyanto, R Oktiani, and R Ragadhita. How to Read and Interpret FTIR Spectroscopy of Organic Material. *Indonesia. J. Sci. Technol*, 4(1):2527–8045, 2019.

[32] C. T Liao and M. H Ho. The Fabrication of Biomimetic Chitosan Scaffolds by Using SBF Treatment with Different Crosslinking Agents. *Membranes*, 1(1):3–12, 2010.

[33] A K Nikolaidis, E A Koulaouzidou, C Gogos, and D S Achilias. Synthesis and Characterization of Dental Nanocomposite Resins Filled with Different Clay Nanoparticles. *Polymers*, 11(4), 2019.